

Hot-dip Galvannealed Steel Sheet of 980MPa Grade Having Excellent Deformability in Axial Crush

Michiharu NAKAYA*¹, Shinjiro KANETADA*¹, Michitaka TSUNEZAWA*²

*¹Sheet & Plate Products Development Department, Research & Development Laboratory, Iron & Steel Business

*²Sheet Products Marketing & Technical Service Department, Iron & Steel Business

Automotive parts that play the roles of energy absorbers must not fracture upon collision. It has been reported that the cracking behavior of a hat-shaped column during an axial crush test correlates with the bending properties of its material and that the conventional hot-dip galvannealed (GA) dual-phase (DP) steel sheets of 980MPa grade have insufficient performance. The newly developed GA 980MPa grade steel sheet with a homogeneous microstructure shows no cracking at a bending angle that would have caused cracking in conventional DP steel sheets, preventing crack propagation in the thickness direction. In order to evaluate the axial crush performance of a part made of the newly developed steel sheet, hat-shaped columns with two different cross-sectional geometries were examined by drop weight impact testing. For both geometries, the newly developed steel exhibited cracks with smaller lengths and higher energy absorption compared with conventional steel.

Introduction

The application of high-strength steel sheets is accelerating in order to reduce the weight of automobiles and improve fuel economy and crashworthiness.¹⁾ The same applies to galvannealed (hereinafter referred to as GA) steel sheets used for underbody parts that require corrosion resistance, and steel sheets with high strength and excellent formability have been developed.^{2), 3)} There are a wide variety of parts to be strengthened, and for the parts around the cabin, materials that can keep the deformation as small as possible are being studied with a view to passenger protection in the event of a collision. In the meantime, materials suitable for members that absorb impact energy by deformation, such as parts in the front and rear of a vehicle, are being studied.⁴⁾ Furthermore, studies are being conducted on steel sheets used for energy-absorbing members. Such steel sheets are required to exhibit no large cracks caused by crushing deformation, as well as to have press formability and weldability. According to these studies, cracks appearing during crushing deformation are highly correlated with indices related to local deformation such as bendability and hole expansibility (index: λ value).⁴⁾⁻⁷⁾

Currently, major 980MPa grade GA steel sheets

are dual phase (hereinafter referred to as DP) steel sheets consisting of ferrite and martensite.⁷⁾ These steel sheets are prone to cracking due to strain concentration at the microstructure boundary and are considered to have limits when it comes to improving bendability and hole expansibility. Thus they are not necessarily suitable for energy-absorbing members. Meanwhile, cold-rolled steel sheets have been developed that, unlike DP steel sheets, have improved hole expansibility and bendability by using a composite structure containing no ferrite.^{9), 10)} Since energy-absorbing members often require corrosion resistance, practical application using GA steel sheets is desired.

Hence, Kobe Steel has developed a 980MPa grade GA steel sheet with a performance suitable for energy-absorbing members. This paper reports the evaluation results of the mechanical properties, bendability and axial crushing properties of the newly developed steel sheet.

1. Characteristics of samples

1.1 Tensile properties and hole expandability

All of the samples were galvannealed steel sheets with a thickness of 1.6 mm. The coating mass was in the range of 45 to 65 g/mm², and the iron concentration in the plating layer was in the range of 7 to 15%. **Table 1** shows the mechanical properties, and **Fig. 1** shows the microstructures.

Table 1 Mechanical properties of sample steels

Sample	Thickness (mm)	YP/YS (MPa)	TS (MPa)	EL (%)	λ (%)
A	1.6	659	1,059	15	17
B	1.6	882	1,004	14	86

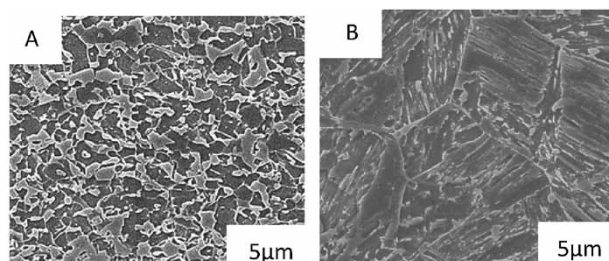


Fig. 1 Typical microstructures of A) DP steel
B) Developed steel

Sample A is DP steel consisting of ferrite and martensite structure. It has low YS characteristics, with λ being slightly less than 20%. Its chemical compositions include C and Mn with the addition of Cr, Mo, etc.

Sample B has a homogeneous microstructure with almost no excessively hard structure, nor soft ferrite; either of these could become a crack initiation point. It is characterized by a high YS and a high hole expandability value compared with Sample A. Its chemical composition includes a decreased amount of C so as to reduce hard structures and hardenability-improving elements to suppress the formation of ferrite.

1.2 Bendability

1.2.1 Bending test method

It has been reported that there is a correlation between cracking behavior and bendability in the axial crush test.^{5), 6)} The German Automobile Manufacturers Association (Verband der Automobilindustrie (VDA)) standard stipulates VDA2380-100 (hereinafter referred to as the "VDA bending test") for evaluating the cracking behavior during member crushing.

In the VDA bending test, a sample placed on a pair of support rolls is bent with a sharp punch (Fig. 2). From the punch load and stroke measured during the test, the bending load-angle diagram (Fig. 3) is created. Since the decrease in load after the maximum load corresponds to crack occurrence, the bending angle at the maximum load (α_{Fmax}) indicates the bending crack limit. In addition, the post uniform slope (PUS), the slope of the straight line connecting the maximum load and the inflection point during the load drop,⁶⁾ is obtained. This slope is related to the propagation of cracks in the sheet thickness direction, and the smaller the slope, the more difficult it is for the cracks to propagate.

Also conducted were a 90° V bending test based

on a general bendability evaluation method. In this test, each test piece is placed on a V-block and bent with a 90° punch having a tip radius of R in the range of 0 to 2.5 mm (0.5 mm pitch). The value R/t was obtained by dividing the minimum bending radius, the smallest radius that caused no cracking, by the sheet thickness, and using that as an index. For both the VDA bending and 90° V-bending, the bending ridge line was made parallel to the rolling direction.

1.2.2 Bending test results

Fig. 4 shows the bending angle vs. load diagram of the VDA bending test and the cross-sectional observation results of a few sample bending angles. Sample A reached the maximum load at a bending angle of 60°, and cracks propagated to half of the sheet thickness in cross-sectional observation at a bending angle of 67°. Sample B, on the other hand, did not crack even at a bending angle of 80°, and

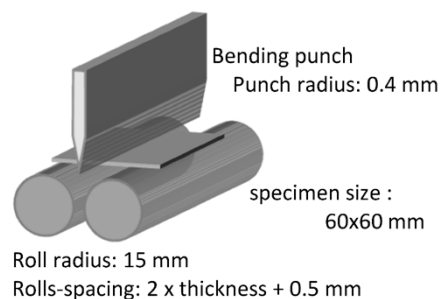


Fig. 2 Set up for VDA bending test

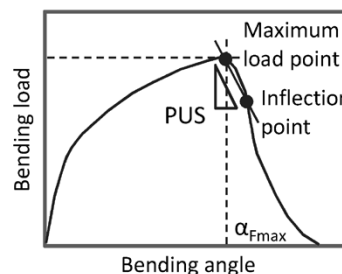


Fig. 3 Bending load-angle curve

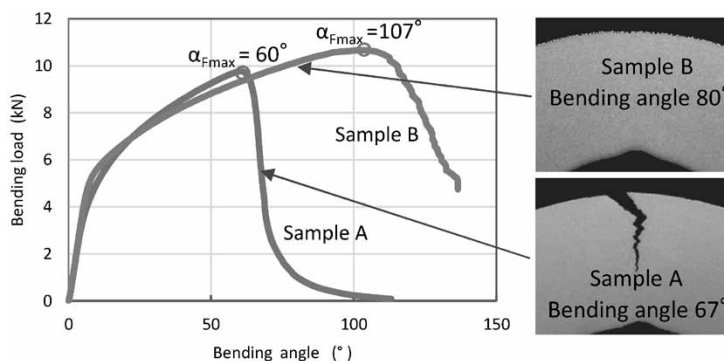


Fig. 4 Bending load-angle curves and cross-sectional observations of samples with bending angles indicated by arrows

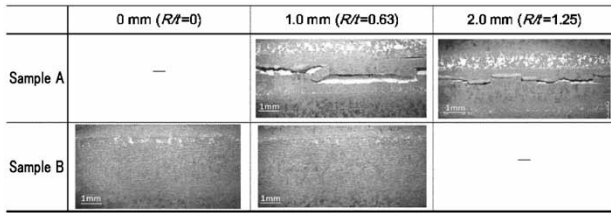


Fig. 5 Appearance of ridge surface after V-bending test

Table 2 Results of bending test

	VDA bending angle (°)	Post uniform slope (MPa)	R/t
Sample A	107	138	1.56
Sample B	60	34	0

the maximum load reached 107°. In the subsequent load reduction process, Sample B showed a slope (PUS) smaller than that of Sample A, and no crack was observed to propagate in the sheet thickness direction.

Fig. 5 shows the observation results of the bending ridge line after the 90° V-bending test. Sample A cracked even for punch $R = 2$ mm, whereas sample B exhibited no crack even when punch $R = 0$ mm.

Table 2 summarizes the results of the above VDA bending test and 90° V-bending test. Sample B shows a favorable value for any index compared with Sample A.

2. Axial crushing characteristics of hat-shaped members

2.1 Test method

The above samples were used to prepare, by bending, two types of columns with hat-shaped cross-sections (type 1 and type 2) (Fig. 6). The column length (perpendicular to the paper surface) was 200 mm, and a backing plate of 590MPa grade cold-rolled high tensile steel (thickness: 1.4 mm) was spot-welded to the column at a spot spacing of 30 mm. On the top and bottom of each column, a steel plate (SS400) with a thickness of 10 mm was arc-welded all around.

A drop weight tester was used for the axial crushing deformation. Each column was fixed to the pedestal on the load cell, and a weight of 190 kg was dropped so that the collision speed was 60 km/h. The weight was stopped at 80 mm after contacting the top of each sample. Two tests were performed for each column and each cross-sectional shape.

In order to quantitatively evaluate the degree of cracking in each sample, crack lengths were measured. The cracks subjected to the measurement were those penetrating the plate thickness. The

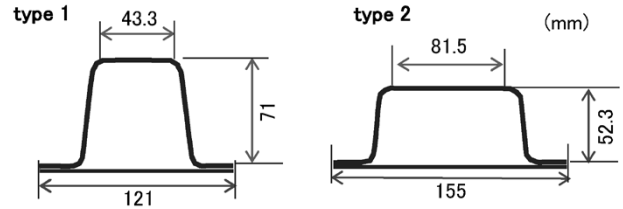


Fig. 6 Cross-sectional geometries of hat-shaped columns

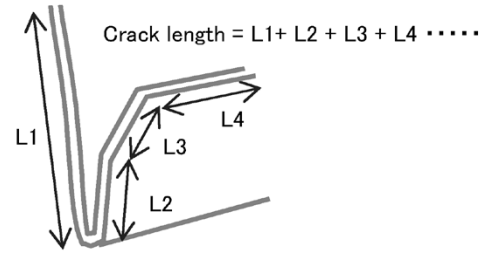


Fig. 7 Method of measuring crack length

fracture surface caused by the axial crushing deformation was identified by visual observation of the outer appearances and half-cut cross-sections of the columns. Next, each fracture surface was divided such that the surface was approximated by straight lines, and the length of each line was measured. The total of these lengths was taken as the fracture surface length (Fig. 7). Although there are two fracture surfaces for one crack, only one of the two fracture surfaces was taken here to avoid duplication, and the fracture surface length was used as the crack length.

2.2 Test results

Fig. 8 shows the absorbed energy vs. displacement curves of the drop weight test. In the case of the type 1 shape, the absorbed energy at the deformation of 80 mm was 8.8 kJ and 9.6 kJ for Sample A, whereas it was 9.7 kJ and 10.1 kJ for Sample B. In the case of type 2, the results were 9.5 kJ and 9.7 kJ for Sample A, and 10.1 kJ and 10.9 kJ for Sample B. For both shapes, Sample B showed higher values.

Fig. 9 include photographs of the appearance of the columns after axial crush. In the columns of Sample A, the ridgeline part was bent at the initial stage of compression to initiate cracks, and the cracks were observed to have propagated along the ridgeline (Fig. 9a)), or to have occurred at the bent part after buckling. (Fig. 9b)). On the other hand, Sample B (Fig. 9c, d)) exhibits no such large cracks. Fig.10 shows the total length of cracks generated during the drop weight tests for each column. Sample A has a large total crack length that may exceed 450 mm at the maximum. On the other hand, that for Sample B was 127 mm at the maximum, and it was found that cracking was suppressed even

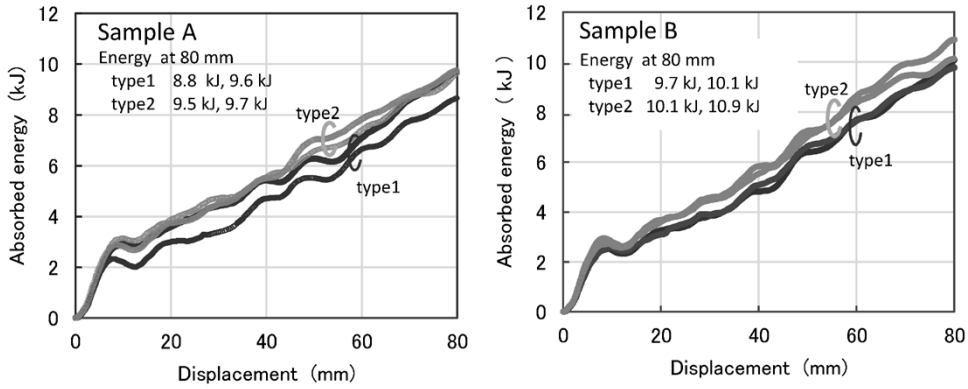


Fig. 8 Absorbed energy vs. displacement curves

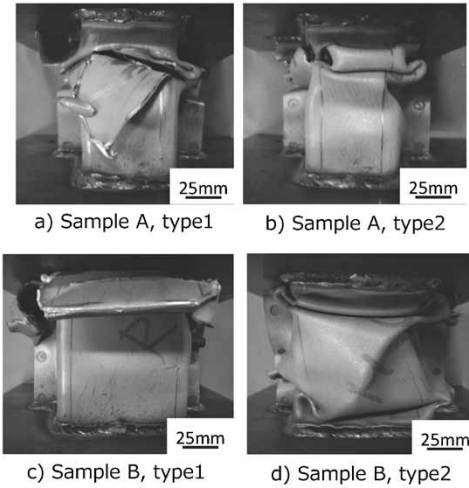


Fig. 9 Appearance of hat-shaped columns after axial crush

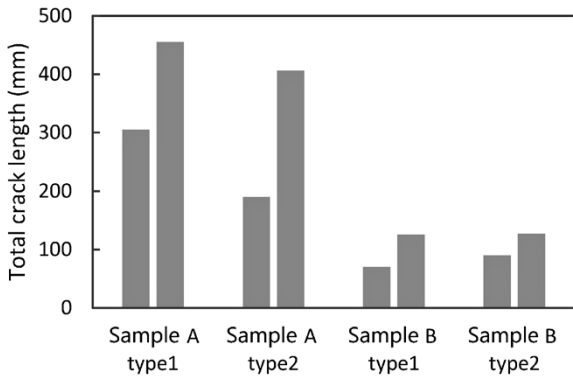


Fig.10 Total crack length in crushed hat-shaped columns

in axial crushing deformation as in the case of the bending test and hole expansion test.

As shown in Fig. 4 (bending angle vs. load diagram), the bending load decreased upon crack occurrence during bending deformation. Even in the case of axial crushing, the deformation load of the entire part may be reduced when cracks occur. A conceivable reason why the absorbed energy of Sample B was higher than that of Sample A is that the decrease in its deformation load due to such

cracking was suppressed, in addition to the high YS of Sample B.

Conclusions

This paper has reported the evaluation results for the mechanical property, bendability, and axial crushing characteristics of GA980MPa grade galvanized steel sheet with homogenous microstructure. This steel sheet exhibited bendability and hole expandability superior to those of the conventional DP steel sheet and was confirmed to suppress the generation of cracks in axial crushing deformation. The newly developed steel sheet is expected to be used widely in the future thanks to its excellent bending workability and stretch flange workability, as well as its advantage in crushing deformation upon collision.

References

- 1) World Auto Steel of World Steel Association Japan Committee. Super Steel, "Advanced High-Ten." Bungeishunju Ltd, 2009, p.10.
- 2) Y. Futamura et al. *R&D Kobe Steel Engineering Reports*. 2011, Vol.61, No.2, p.41.
- 3) M. Ikeda et al. *R&D Kobe Steel Engineering Reports*. 2017, Vol.66, No.2, p.8.
- 4) H. Maki et al. *IJAE*. 2017, Vol.48, No.66, p.1347.
- 5) P. Larour et al. International Deep Drawing Group, IDDRG International Conference 2010. Graz, Austria, 2010, 0531/06-02.
- 6) J. Naito et al. *R&D Kobe Steel Engineering Reports*. 2017, Vol.66, No.2, p.69.
- 7) S. Chinzei et al. *R&D Kobe Steel Engineering Reports*. 2017, Vol.66, No.2, p.76.
- 8) World Auto Steel of World Steel Association Japan Committee. Super Steel, "Advanced High-Ten." Bungeishunju Ltd, 2009, p.18.
- 9) M. Miura et al. *R&D Kobe Steel Engineering Reports*. 2009, Vol.57, No.2, p.15.
- 10) M. Nakaya et al. *R&D Kobe Steel Engineering Reports*. 2009, Vol.59, No.1, p.49.